Robust Limit Cycle Control in an Attitude Control System with Switching-Constrained Actuators

Alexandre Rodrigues Mesquita[1*], Karl Heinz Kienitz[1] and Erico Luis Rempel[2]

***Abstract*— In this paper the robust behavior in some piecewise affine systems with minimally spaced transition times is studied. Such systems are found e.g. in satellites and satellite launchers. On-off thrusters are frequently used as actuators for attitude control and are typically subject to switching constraints. In these systems, persistent motions of different nature may occur, such as limit cycles, quasi-periodic-like and chaotic motions. In the presence of model uncertainties, the emergence of bifurcations in these systems can seriously affect performance. In this contribution, model uncertainties in the actuation device are evaluated in both a structured and an unstructured fashion. Then, Tsypkin's method is used to investigate the robustness of the condition for of limit cycles. Robustness frontiers in the space of control parameter are identified. These frontiers are verified via simulation and compared to that given by the describing function method, revealing the difficulties of this latter method to address the robustness analysis in this system. Moreover, we present a design method for robust controllers based on the Hamel locus. An evaluation of performance requirements such as fuel consumption, limit cycle amplitude and transient response is carried out in the identified regions of robust behavior. Thus, we are able to design robust controllers that efficiently exploit the switching-constrained actuators.**

I. INTRODUCTION

Throughout the last decades, attitude control systems with switching actuators have been used in satellite and launching systems [1], [2], [3], [4], [5]. In the attitude stabilization phase, such systems typically have been operated in limit cycle conditions. As actuators, several types of on-off thrusters are employed, such as hydrazine, cold-gas and pulsed plasma thrusters [2]. These thrusters are typically affected by switching constraints, which have been a cause of concern about the degradation of the system's performance. As shown by Oliveira and Kienitz [4], non-conventional analysis/design problems arise when actuators are subject to switching-time restrictions. Certain conditions ensure that limit cycles exist. When these conditions do not hold, system motion may not be of limit cycle type.

During recent research on the issue of limit cycle control for a system with minimally spaced switching-times, we observed [6] that the optimal control parameter set, which guarantees minimum amplitude and minimum fuel consumption, lies on the frontier where the system bifurcates into nonperiodic persistent motions. Here arises the concern with the robustness of an optimal controller. In this paper, we are interested in the design of robust controllers that preserve a good performance while guaranteeing operation in the limit cycle mode, i.e., controllers that mitigate the possibility of bifurcations.

Computing the limit cycle points of uncertain nonlinear systems has attracted the attention of researchers in the last decade. Most of them were simply concerned with the inhibition of limit cycles in order to prove stability. In the main papers available on this issue [7], [8], [9], [10], [11], [12], [13], [14], first harmonic approximation has been adopted. The deficiency of this approximated analysis for the studied system was shown in [6].

In [7] Tierno applies a rational approximation to the describing function of the nonlinear element, and incorporates describing function analysis into a generalized structured singular value (μ) framework of robustness analysis. Fadali and Chachavalvoong [8] and Huang et al. [9] employed Kharitonov's theorem to the limit cycle existence condition given by the describing function method. The same condition is analyzed by Nataraj and Barve [10], who propose an algorithm based on interval analysis to construct the limit cycle locus of nonlinear systems with separable nonlinearities in the presence of parametric uncertainties in the linear and nonlinear elements. Tan and Atherton [11] present a method to compute magnitude and phase envelopes of uncertain transfer functions and apply describing function analysis to predict the existence of limit cycles. This approach is the closest to the one we present in this paper. Alternatively, washout filters were proposed to ensure preservation of limit cycle amplitude and shape [12].

The most consistent approach is due to Katebi and Zhang [14]. They apply a μ-based analysis method to systems with norm-bounded perturbations in the linear part and incorporate the dynamics neglected by the describing function approximation as an unstructured uncertainty into the problem description. Leephakpreeda [13] proposes a similar H_∞-based control approach to predict limit cycles for fuzzy control systems. Nevertheless, these approaches are not useful when dealing with some relay-type nonlinearities, for the uncertainty due to the approximation may be conservative to the point that a robust controller result may not exist. A natural conclusion is that the intended robustness analysis is hardly possible without considering higher-order harmonics. Hence, in this contribution we consider exact methods for limit cycle prediction. Using Tsypkin's method, we are able to address both parametric uncertainties and magnitude-phase envelopes of uncertain transfer functions. By analyzing

[2] Departamento de Matemática, Instituto Tecnológico de Aeronáutica, CTA, São José dos Campos, 12228-900, Brazil

[1] Departamento de Sistemas e Controle, Instituto Tecnológico de Aeronáutica, CTA, São José dos Campos, 12228-900, Brazil

*A. Mesquita acknowledges financial support from Fundação de Amparo à Pesquisa do Estado de São Paulo (FAPESP).

each point in a grid of the space of control parameters, we can find a frontier that determines robust limit cycle behavior and, as a consequence, we are able to avoid nonperiodic regimes as we are looking for an amplitude minimization. On this frontier, we calculate an interval of amplitude variation and study the vanishing of transients. In addition, we propose a design using a Hamel-type locus, which allows a decrease in the dimension of the space of control parameters.

II. PROBLEM DESCRIPTION

The problem description given here is akin to that in [4]. Consider a simple rigid body (e.g. satellite or rocket in the upper atmosphere) whose attitude ϕ is to be controlled using sets of small thrusters, which are on-off actuators with switching-time restrictions. A simplified representation of the system is shown in Fig. 1, where the thrust F may assume final values $-F_{\max}$, 0 or $F_{\max}$.

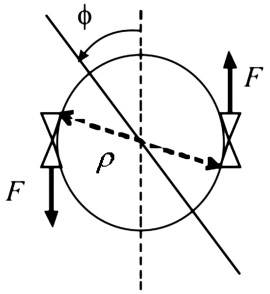

Fig. 1. Rigid body with a set of thrusters

A body inertia $J = 1500$ [kgm^2] is given. The small thruster actuators do have delays and switching-time restrictions:

- Maximum absolute torque: $\rho F_{\max} = 308$ [Nm].
- Thrust build up dynamics (On):
  - 10% of maximum thrust: 10-30 [ms]
  - 90% of maximum thrust: 20-50 [ms]
- Thrust build up dynamics (Off):
  - 90% of maximum thrust: 9-16 [ms]
  - 10% of maximum thrust: 15-50 [ms]
- Switching-time restrictions:
  - minimum duration of pulses: $t_{\text{on}} = 100$ [ms].
  - minimum rest between successive pulses of the same sign: $t_{\text{s}} = 50$ [ms].
  - minimum rest between pulses of different sign: $t_{\text{off}} = 500$ [ms].

The typical requirement for the controlled system is that initial conditions and attitude perturbations shall asymptotically die away into a well behaved limit cycle. For the purpose of achieving an appropriate performance, a tachometric feedback law (feedback of position and velocity) and a single-pole controller $C(s) = \frac{1}{s-p}$ are added to the loop, resulting in the controlled system represented in Fig. 2.

The Actuators block of Fig. 2 is decomposed into a series structure with two sub blocks. The first one contains a relay with the above switching restrictions and with output

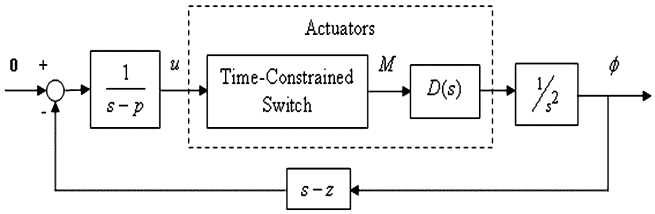

Fig. 2. Block diagram of the controlled system

in $\{k_r, -k_r, 0\}$, where $k_r = F_{\max}\rho/J$. The second one contains a linear dynamics which models thrust build up. In practice, actuator delays may vary during the operation of the system. Their value may depend on several parameters. Thus, the model is affected by uncertainty. All the gains in the system are rearranged to the output M of the Time-Constrained Switch block. Since the controller is linear, these gains affect only the amplitude of the response.

According to relay systems theory, for appropriate values of p and z, we should expect symmetric unimodal limit cycle behavior. Necessary conditions to the existence of this limit cycle can be provided either by approximate or exact methods (see [15]). The above switching-time restrictions impose another condition, which states the existence of a maximum value for the switching frequency f:

$$f \leq f_{\max} = \frac{1}{2(t_{\text{on}} + t_{\text{off}})} \tag{1}$$

Since the controller is linear, the period for which the actuator is off at each half-cycle is always t_{off}. Thus, the fuel consumption will be minimum if the period for which the actuator is on is also minimum, that is, if the limit cycle frequency is maximum. Additionally, if we calculate $\phi(t)$ approximately by double-integrating the periodic train of pulses $M(t)$, one can intuitively see that the amplitude decreases monotonically with f as well. However, if the controller demands a switching frequency higher than $f_{\max}$, nonperiodic persistent motions arise [6] and the amplitude may vary significantly in the presence of uncertainties. In [16], we characterize a quasi-periodic-like motion that arises as a bifurcation from periodic motion.

Hence, the robust performance aimed in this paper consists of the occurrence of single-switching (unimodal) limit cycles that possess a set of possible frequencies with upper bound $f_{\max}$ and maximum lower bound.

III. AN EXACT METHOD FOR PREDICTING LIMIT CYCLES

In this section we obtain necessary conditions to the existence of limit cycles in the fashion followed by Tsypkin [17]. Suppose the existence of a single-switching (unimodal) periodic output $M(t)$ with period T as depicted in Fig. 3.

As noted in [4], this wave is equivalent to the sum of a square wave with amplitude $k_r/2$ and another square wave with the same amplitude but delayed by t_{off}. If we call $\omega_0 =$

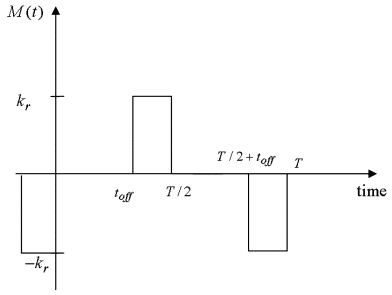

Fig. 3. Unimodal periodic actuators' output

$2\pi T^{-1}$, the following Fourier series decomposition can be verified:

$$M(t) = \sum_{k \text{ odd}} \frac{4k_r}{\pi k} \Im \left\{ \left(\frac{1 + e^{-jk\omega_0 t_{\text{off}}}}{2} \right) e^{jk\omega_0 t} \right\} \quad (2)$$

Thus, in the case of single-switching periodic motion, the Time-Constrained Switch block can be replaced by a simple relay with output $M'(t)$ in $\{k_r, -k_r\}$ and followed by the transfer function $\left(1 + e^{-st_{\text{off}}}\right)/2$.

Two necessary conditions to the existence of such output will be considered, see [17, Eq. 5.47]:

$$\begin{aligned} u(T/2) &= 0 \\ \frac{du}{dt}(T/2) &< 0 \end{aligned} \quad (3)$$

These conditions are not sufficient because we do not take into account the possibility of intermediary crossings $u(t) = 0$ for $t < T/2$. The Tsypkin locus is defined in [17, Eq. 6.1] by

$$\Lambda(\omega) = \frac{1}{\omega} \frac{du}{dt}(T/2) + ju(T/2) \quad (4)$$

According to the conditions in Eq. (3), the existence of a limit cycle of angular frequency ω_0 requires that $\angle\Lambda(\omega_0) = \pi$. Defining the transfer function $L(s) = -U(s)/M'(s)$ and recurring to Eqs. (2) and (4), we can verify the following expression for the Tsypkin locus

$$\Lambda(\omega) = \sum_{k \text{ odd}} \frac{4k_r}{\pi} \left[\Re\{L(j\omega k)\} + j\frac{1}{k} \Im\{L(j\omega k)\} \right] \quad (5)$$

Thus, the Tsypkin locus is a useful tool for the determination of limit cycle properties such as frequency and amplitude. Though other exact methods exist, such as the state-space based method [18], Tsypkin's is a more convenient method when dealing with uncertain systems, since it is more convenient to express uncertainties in the frequency domain. A useful criterion to address the limit cycle stability graphically from the Tsypkin locus is provided by the following necessary condition from [17, Eq. 10.69]:

$$\Im \left\{ \frac{d\Lambda(\omega)}{d\omega} \right\} > 0 \quad (6)$$

Another useful result from [17, Eq. 6.54] is the exact expression of the Tsypkin locus in the case the transfer function from the relay output to the relay input has the form:

$$L(s) = \frac{P(s)}{s^2 Q(s)} e^{-s\tau} \quad (7)$$

where $P(s)$ and $Q(s)$ are polynomials with non-zero simple roots.

This expression is applied in the parametric robustness analysis and is also interesting since it provides qualitative knowledge on the Tsypkin's locus, such as the maximum number of possible limit cycles.

Notice that, there was not a minimal pulse duration, a limit cycle with frequency $\omega_0 = \pi/t_{\text{off}}$ would exist, since $\Lambda(\pi/t_{\text{off}}) = L(\pi/t_{\text{off}}) = 0$. At this frequency, however, the output $M(t)$ is always zero, that is, this limit cycle is an equilibrium point at the origin. If this limit cycle was proved to be stable, the system could be stabilized by the application of infinitesimal duration pulses. As these pulses are not allowed, an undesirable quasi-periodic-like motion would arise.

A second remarkable limit cycle is that occurring when ω approaches zero. Indeed, the double integrator in $L(s)$ implies that $\lim_{\omega \to 0^+} \angle\Lambda(\omega) = \lim_{\omega \to 0^+} \angle L(\omega) = \pi$. If this limit cycle is stable, there will be trajectories with no switching at all, that is, there will be instability.

IV. MODEL UNCERTAINTIES

This section discusses two representations of the family of possible systems that correspond to the real system. We consider both structured and unstructured representations. A parametric representation is useful because truncation errors can be suppressed through the use of the exact expression for the Tsypkin locus and, chiefly, because it allows validating results via simulation. On the other hand, an unstructured formulation is more inclusive and demands a lower computational effort.

Two of the main uncertainties in the adopted model reside in the values of J and F, which may vary with time because of propellant consumption and atmospheric pressure decrease. Since the controller is linear, it is clear that these parameters do not affect the kind of motion performed by the system but for its amplitude, which is proportional to them. Another source of uncertainty is the coupling of the roll angle with other modes.

In this paper we consider only the uncertainty present in the thrust build up dynamics, since the first uncertainty mentioned is too simple to analyze and the second one is too difficult and of little relevance. Moreover, we assume that the time variation of J and F is low enough so that we can consider a limit cycle type motion.

Though build up dynamics are different when actuators switch on or off, they are dynamically alike and their

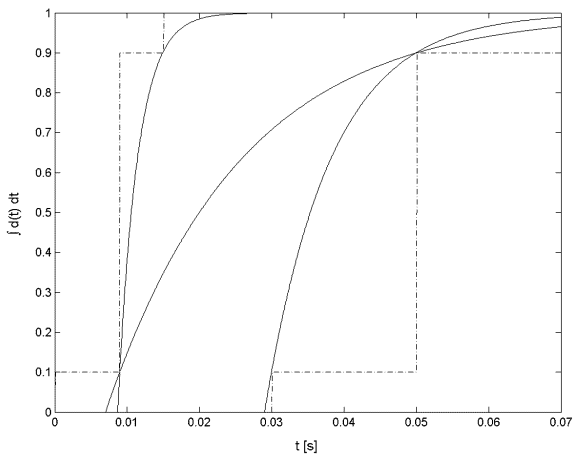

Fig. 4. Thrust build up envelope (dashed) and extreme curves for $D(s) = D(\alpha, \tau, s)$ (solid)

settling times are much less than t_{off}. Under these conditions, one can verify that assuming symmetric build up dynamics will just make our robustness analysis more conservative. Therefore, we model these dynamics by the transfer function $D(s)$, whose step response must be contained in a time envelope given by the fastest and the slowest responses that we describe in section II.

Next, we derive a parametric representation of the possible $D(s)$. Let us denote by $D_F(s)$ and $D_G(s)$ the transfer functions related, respectively, to the fastest and to the slowest curves in this envelope. Figure 4 depicts this envelope and the extreme curves that fit in it and whose related transfer functions have the form

$$D(\alpha, \tau, s) = \frac{e^{-s\tau}}{\alpha s + 1} \tag{8}$$

These curves are designed to graze the vertices of the envelope and are unique in what concerns this feature. For the approximation $D_F^a(s)$ of the fastest response, we found $\alpha_F = 2.73$ [ms] and $\tau_F = 8.71$ [ms]. For the approximation D_G^a of the slowest response, $\alpha_G = 9.10$ [ms] and $\tau_G = \tau_{\max} = 29.04$ [ms]. For the minimum band transfer function $D_{FG}^a(s)$, we found $\alpha_{\max} = 18.66$ [ms] and $\tau_{\min} = 7.03$ [ms]. We must note that, among the most simple classes of transfer functions, $D(\alpha, \tau, s)$ is that which best approximates the content of the envelope. In fact, no response from a rational second order transfer function fits in it.

For the minimum value of α, we assume $\alpha_{\min} = \alpha_F = 2.73$ [ms]. Then, it is possible to establish an interesting parameter domain observing the condition that at least 90% of total thrust is attained for $t = 50$ [ms]. This domain is given by $\tau \in [\tau_{\min}, \tau_{\max}]$ and $\alpha \in \left[\alpha_{\min}, \frac{\tau - 0.05}{\ln 0.1}\right]$.

In the following lines we derive an unstructured formulation of uncertainties leading to magnitude and phase envelopes in frequency domain. Figure 5 exhibits the frequency response of the above transfer functions for the frequency band of interest. Given that in the largest extent of this band we have $|D(j\omega)|$ very close to 1, we conclude that the magnitude envelope will play a role of minor importance in the determination of limit cycles. Hence, we simply adopt the bounds given by the parametric characterization: $|D_F^a(j\omega)|$ and $|D_{FG}^a(j\omega)|$.

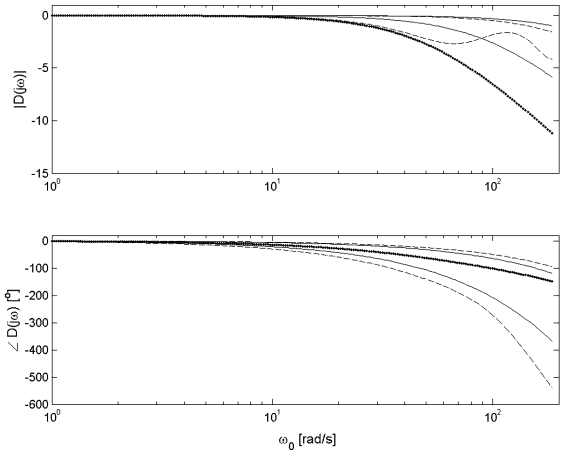

Fig. 5. Bode plots for $D_F(s)$ and $D_G(s)$ (dashed), for the approximations $D_F^a(s)$ and $D_G^a(s)$ (solid), and for $D_{FG}^a(s)$ (black dots)

In order to determine a phase envelope, we assume that thrust build up curves increase monotonically and have a settling time τ_a. Then, we must have a impulse response $d(t) \geq 0$ for $0 \leq t < \tau_a$ and $d(t) = 0$ for $t \geq \tau_a$. Thus,

$$\begin{aligned} D(j\omega) &= \int_0^{\tau_a} d(t) e^{-j\omega t} dt \\ &\Rightarrow \angle D(j\omega) \in [-\omega\tau_a, 0] \end{aligned} \tag{9}$$

Moreover, denoting by $r(t)$ the step responses and recalling that $r(t) \leq r_F(t)$ for $0 \leq t \leq \tau_a$ and $r(t) = r_F(t)$ for $t \geq \tau_a$, we obtain

$$\begin{aligned} &D(j\omega) - D_F(j\omega) = j\omega \int_{-\infty}^{\infty} [r(t) - r_F(t)] e^{-j\omega t} dt \\ &= j\omega \int_0^{\tau_a} [r(t) - r_F(t)] e^{-j\omega t} dt \\ &\Rightarrow \angle(D(j\omega) - D_F(j\omega)) \in \left[-\frac{\pi}{2} - \omega\tau_a, -\frac{\pi}{2}\right] \end{aligned} \tag{10}$$

Similarly,

$$\angle(D(j\omega) - D_G(j\omega)) \in \left[\frac{\pi}{2} - \omega\tau_a, \frac{\pi}{2}\right] \tag{11}$$

Now we use the fact: if $\angle a \in [\underline{\varphi}, \bar{\varphi}]$, $\angle b \in [\underline{\chi}, \bar{\chi}]$ and $\bar{\chi} < \underline{\varphi} + \pi$, then $\angle(a + b) \in \left[\min\{\underline{\varphi}, \underline{\chi}\}, \max\{\bar{\varphi}, \bar{\chi}\}\right]$. Applying this result to the sum of $D(j\omega) - D_F(j\omega)$ and $D_F(j\omega)$ we may conclude that, as long as $-\pi/2 < \angle D_F(j\omega) < \pi/2 - \omega\tau_a$,

$$\angle D(j\omega) \leq \angle D_F(j\omega) \tag{12}$$

By an analogous reasoning, for $-\pi/2 < \angle D_G(j\omega) < \pi/2 - \omega\tau_a$, we assert that

$$\angle D_G(j\omega) \leq \angle D(j\omega) \tag{13}$$

Therefore, there is an interval for which we can use $\angle D_F(j\omega)$ and $\angle D_G(j\omega)$ as bounds of the phase envelope. Outside this interval, we adopt the boundaries given by Eq. (9). Taking $\tau_a = 65$ [ms], we have the limit transfer functions of the frequency domain envelopes:

$$\bar{D}(j\omega) = \begin{cases} \left|\frac{1}{\alpha_{\min} j\omega + 1}\right| \frac{D_F(j\omega)}{|D_F(j\omega)|} & \text{, if } \omega < 28 \\ \left|\frac{1}{\alpha_{\min} j\omega + 1}\right|, & \text{, if } \omega \geq 28 \end{cases} \tag{14}$$

$$\bar{D}(j\omega) = \begin{cases} \left|\frac{1}{\alpha_{\max} j\omega + 1}\right| \frac{D_G(j\omega)}{|D_G(j\omega)|} & \text{, if } \omega < 30.5 \\ \left|\frac{1}{\alpha_{\max} j\omega + 1}\right| e^{-j\omega\tau_a}, & \text{, if } \omega \geq 30.5 \end{cases} \tag{15}$$

V. LIMIT CYCLE ROBUSTNESS ANALYSIS

In this section we test the necessary conditions for the existence of limit cycles with respect to their robustness. Since these conditions are necessary only, we validate them via simulation. The robust controller to be designed is that for which the supremum of the set of predicted possible frequencies is not larger than $\omega_{\max} = 2\pi f_{\max}$, in such a way that Eq. (1) is respected. Therefore, a bifurcation frontier in the space of control parameters can be calculated by checking for values of z and p such that this supremum is ω_{max}. Let $\mathcal{B}$ be the family of possible Tsypkin loci for the uncertain system and assume that $\Re\{\Lambda_\xi(\omega_{\max})\} < 0$ for all $\Lambda_\xi \in \mathcal{B}$. Then, the periodic to quasi-periodic-like bifurcation frontier must lie on the curve

$$(z, p) : \min_{\Lambda_\xi \in \mathcal{B}} \{\Im\{\Lambda_\xi(\omega_{\max})\}\} = 0 \tag{16}$$

As shown in Fig. 6, a point of the bifurcation frontier occurs whenever the lower bound of the interval of possible $\Im\{\Lambda(\omega_{\max})\}$ crosses zero. However, the bifurcation frontier may not coincide with the above curve, given that we do not verify sufficient conditions for the existence of stable limit cycles.

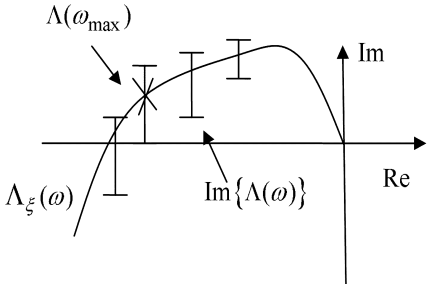

Fig. 6. Uncertain Tsypkin locus for p and z on the bifurcation frontier

In the case of parametric uncertainties, the bifurcation frontier is calculated by the evaluation of the exact Tsypkin locus expression in a grid of the parameter space. We have adopted $\Delta\alpha = 0.8$ [ms] and $\Delta\tau = 1.1$ [ms]. For each combination of z and p, if we find $\Im\{\Lambda_\xi(\omega_{\max})\} < 0$, we may interrupt the search and conclude that the limit cycle is not robust at this point. In fact, as $\Lambda_\xi(\pi/t_{\text{off}}) = 0$ and $\pi/t_{\text{off}} > \omega_{\max}$, we should expect the Tsypkin locus to cross positively the real axis for $\omega > \omega_{\max}$, which violates the condition in Eq. (1).

In the case of unstructured uncertainty, we can establish a lower bound for $\min_{\Lambda_\xi \in \mathcal{B}} \{\Im\{\Lambda_\xi(\omega_{\max})\}\}$ by choosing $D(j\omega) = D_{\xi^*}(j\omega)$ inside the phase and magnitude envelopes in such a way that each harmonic contribution to $\Im\{\Lambda(\omega_{\max})\}$ in Eq. (5) is minimized. Figure 7 illustrates the determination of $L_{\xi^*}(j\omega)$. At each frequency, the set of possible $D(j\omega)$ has rectangular shape and the worst case $L(j\omega)$ is given by the point on its boundary with the largest magnitude and with phase as close as possible to -90°. Calculating $D_{\xi^*}(j\omega)$ as proposed, for some typical values of p and z, we can observe that it coincides with $\bar{D}(j\omega)$ for frequencies below $\omega_{\max}$ and for other frequency intervals whose total length surpasses a half of the focused frequency band. Additionally, we observe that $D_{\xi^*}(j\omega)$ is subject to very strong variations, which suggests that $D_{\xi^*}(s)$ is not a rational transfer function and that its step response may even not be contained in the time envelope. However, since the worst case $\Lambda(\omega)$ depends only on D_{ξ^*} at the odd harmonics $k\omega_{\max}$, a simpler $D_{\xi^*}(j\omega)$ becomes possible and fast dynamics seem to predominate in it. In the case of $p = -5$ and $z = -9$, for instance, the transfer function $\bar{D}(j\omega)$ is practically equal to $D_{\xi^*}(j\omega)$ until the ninth harmonic.

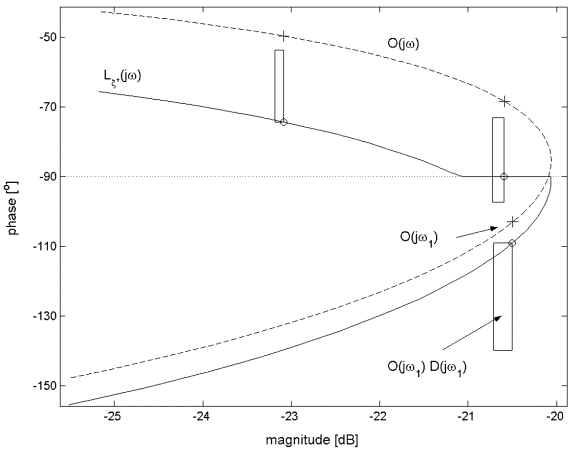

Fig. 7. Example of the determination of the worst case $L(j\omega) = O(j\omega)D(j\omega)$

A. HAMEL'S METHOD ANALYSIS

In this section we present an alternative analysis method that can be useful in synthesis. It employs the Hamel locus, which allows for a more intuitive zero allocation. If we define $\epsilon = u(T/2)$ and $\dot{\epsilon} = \frac{du}{dt}(T/2)$, the Hamel locus is given by the curve in the phase plane:

$$H = (\epsilon, \dot{\epsilon}) = (\omega\Re\{\Lambda\}, \Im\{\Lambda\}) \tag{17}$$

The oscillation frequency is also determined by the crossing of the abscissa. On the other hand, we can interpret the placing of a block $(s-z)$ in the open loop as a change in the switching condition from $\epsilon = 0$ to $-z\epsilon + \dot{\epsilon}$. Therefore, the oscillation frequency can be found in the crossing of the line $\epsilon = \dot{\epsilon}/z$ by the Hamel of the system without the zero. This suggests that a robust controller synthesis can be done by the proper allocation of a line passing through the origin and tangent to the set of possible Hamel locus points at $\omega = \omega_{\max}$. If we consider this set to be rectangular and that $H(\omega_{\max})$ belongs to the second quadrant, we conclude

$$z = \frac{\min \epsilon(\omega_{\max})}{\min \dot{\epsilon}(\omega_{\max})} = \omega_{\max} \frac{\min \{\Re\{\Lambda_\xi(\omega_{\max})\}}{\min \{\Im\{\Lambda_\xi(\omega_{\max})\}} \tag{18}$$

The above procedure is illustrated in Fig. 8. Since one considers a rectangular set of possible $H(\omega_{\max})$, this procedure is expected to be somewhat more conservative than that we present using the Tsypkin's method.

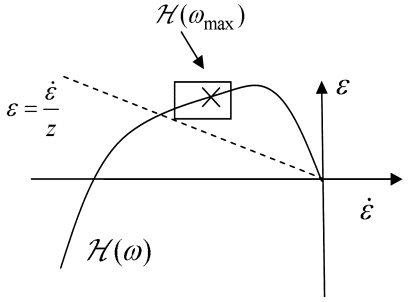

Fig. 8. Robust design by allocation of the switching line (dashed) on the Hamel locus (solid)

B. INSTABILITY FRONTIER

Besides the periodic to quasi-periodic-like bifurcation frontier, we can identify another important frontier given by the arising of instability. Based on Eq. (6), the instability frontier is expressed as follows:

$$(z,p) : \max_{\Lambda_\xi \in \mathcal{B}} \left(\lim_{\omega \to 0^+} \Im \left\{ \frac{d\Lambda_\xi}{d\omega}(\omega) \right\} \right) = 0 \tag{19}$$

For each combination of z and p on the frontier, we must have $\lim_{\omega\to 0^+} \Im\left\{\frac{d\Lambda_\xi}{d\omega}(\omega)\right\} = 0$ in the worst case, which occurs if and only if $\lim_{\omega\to 0^+} \Im\left\{\frac{dL_\xi}{d\omega}(\omega)\right\}$. As $L_{\xi^*}(j\omega) \to \pi$ in the limit, the above condition is equivalent to

$$\lim_{\omega \to 0^+} \frac{d\angle L_{\xi^*}}{d\omega}(j\omega) = 0 \tag{20}$$

Replacing $L_{\xi^*}(j\omega)$, we obtain

$$\frac{d\angle L_{\xi^*}}{d\omega}(j\omega) = \frac{d}{d\omega}\angle \left(-\frac{j\omega - z}{\omega^2(j\omega - p)} \frac{1 + e^{-j\omega t_{\text{off}}}}{2} D_{\xi^*}(j\omega) \right)$$
$$= \frac{d}{d\omega}\left(\pi - \arctan\frac{\omega}{z} + \arctan\frac{\omega}{p} - \frac{\omega t_{\text{off}}}{2} \right) + \frac{d}{d\omega}\angle D_{\xi^*}(j\omega) \tag{21}$$

Taking the derivative and the limit, we obtain for Eq. (20)

$$\frac{1}{p} - \frac{1}{z} - \frac{t_{\text{off}}}{2} + \lim_{\omega \to 0^+} \frac{d}{d\omega}\angle D_{\xi^*}(j\omega) = 0 \tag{22}$$

According to the phase envelope, the limit above must be in the interval [-53,-8.7] [ms]. In the case of parametric uncertainties, the limit is given by $-(\alpha+\tau)$, where $-(\alpha+\tau) \in [-38.1, -9.8]$ [ms], that is contained by the interval for unstructured uncertainty. As the derivative of the phase and of the imaginary part of $L_{\xi^*}(j\omega)$ have opposite signs in the limit $\omega \to 0^+$, we conclude that the instability frontier is determined by Eq. (22) with $D_{\xi^*}(j\omega)$ being such that $\lim_{\omega\to 0^+} \frac{d}{d\omega}\angle D(j\omega)$ is minimum.

VI. NUMERICAL RESULTS

The numerical assessment considers the space $z \times p = [-3, 0] \times [-60, -10]$ with grid resolution $\Delta z \times \Delta p = 0.2 \times 0.1$. The choice of the number N of harmonics in the truncation of the Tsypkin locus expression is empirical. In Fig. 9 we exhibit the bifurcation frontier given by Hamel locus approach for different N. From this we decided to adopt $N = 27$. The figure also indicates that a first order approximation would seriously affect a robust design.

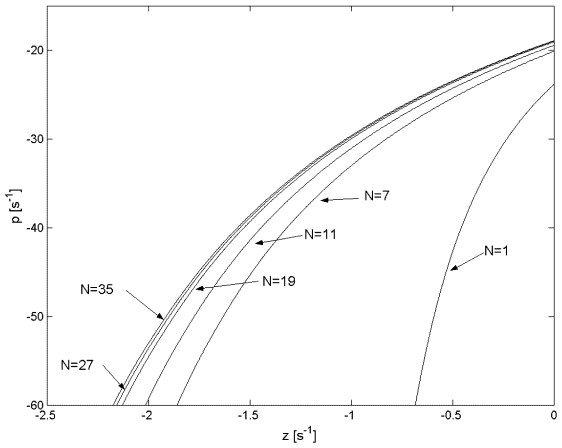

Fig. 9. Convergence of the bifurcation frontier as the truncation term N is increased

Figure 10 exhibits the regions where the limit-cycle frequency is robustly bounded. The region for proper control is that where $0 < \omega_0 < \omega_{\max}$. Especially, the amplitude is minimized on the bifurcation frontier and increases indefinitely as we move towards the instability frontier. We should remark that for $z > 0$ limit cycles become unstable. In fact, when z changes sign the residue of the term $1/s^2$ in $L(s)$ also changes sign, which makes unstable the related closed-loop sampled-data system we use to assess limit cycle stability, as done in [17, Chapter 10].

In order to evaluate the conservativeness of this frontier we compare it with frontiers given by other approaches in Fig. 11. The parametric analysis is carried on the domain of z and p with grid resolution $\Delta\alpha = 0.8$ [ms] and $\Delta\tau = 1.1$

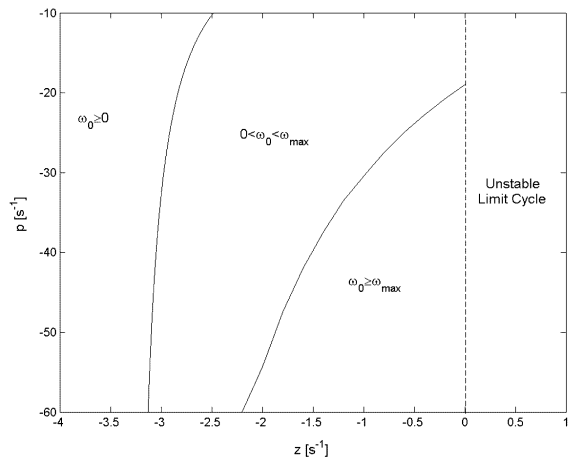

Fig. 10. Regions of robust limit cycle behavior (unstructured uncertainty)

[ms]. We compare the frontier obtained for the unstructured uncertainty to the one for the structured uncertainty. On the p axis the second curve may be at most 12 [s^{-1}] below the first one; in the z axis, at most 0.4 [s^{-1}] to the right. It is remarkable that the worst case $\Lambda_\xi(\omega_{\max})$ is always verified for the case of fastest thrust build up, that is, for $\alpha = \alpha_{\min}$ and $\tau = \tau_{\min}$. The frontier provided by the Hamel locus design was slightly more conservative than that given by unstructured uncertainties. On the p axis they differ at most by 1 [$s^{-}1$]; on the z axis, by 0.04 [$s^{-}1$]. At length, we trace the frontier obtained when we consider $D(j\omega) = D_F(j\omega)$. This frontier suggests that the envelope technique is an important cause of conservativeness, otherwise we would have the curve for $D_F(j\omega)$ closer to the frontier given by the unstructured uncertainty than to that given by parametric uncertainties.

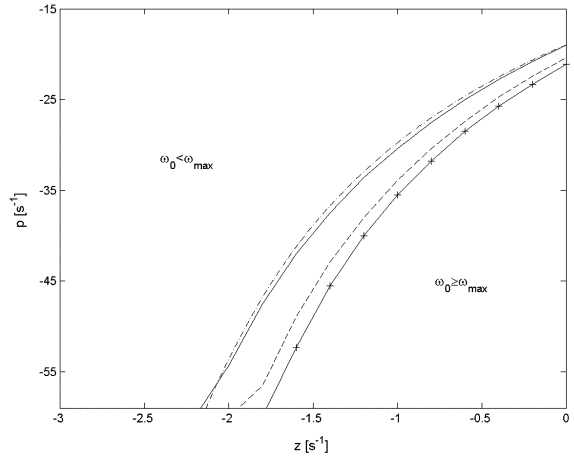

Fig. 11. Comparison of the bifurcation frontiers based on unstructured uncertainty (solid), on parametric uncertainties (cross), on the function $D_F(s)$ (dashed) and on Hamel locus approach (dot-dashed)

The large area of the region in Fig. 10 where $0 < \omega_0 < \omega_{\max}$, suggests that the desired robust controller will be subject to great intervals of frequency and amplitude variation. Figure 12 shows the variation of the minimum possible frequency along the bifurcation frontiers given by parametric and nonparametric approaches. In order to obtain this curve, we have employed the exact Tsypkin locus expression and executed a parametric search over α and τ for each point on the frontiers. Note that minimum frequencies have always been verified for the case of slowest thrust build up, that is, for $\alpha = \alpha_G$ and $\tau = \tau_G$.

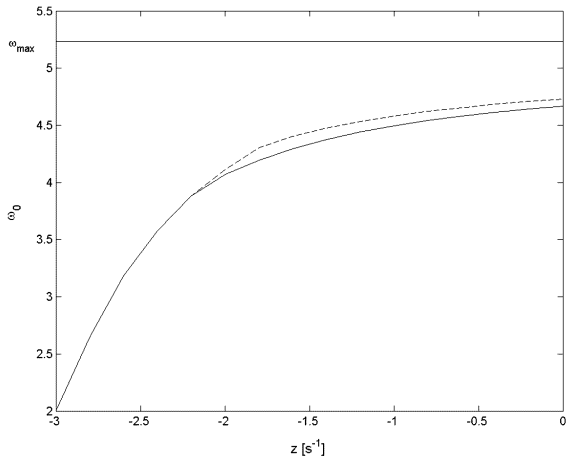

Fig. 12. Minimum oscillation frequency varying along the bifurcation frontiers given by parametric (dashed) and nonparametric (solid) approaches

As one could expect, the largest intervals of amplitude variation occur nearby the instability frontier and the smallest intervals occur in the limit cycle stability boundary at $z = 0$. Notice that the parametric approach, being less conservative, provides a little smaller interval. Choosing z in order to have a minimum amplitude variation has obviously a drawback, since in this case the limit cycle would be marginally stable. This drawback is the duration of transient responses, which increases unboundedly as z approaches 0. The maximum value of the roll angle amplitude settling time for 1% was obtained via simulation and plotted in Fig. 13. Thus, the designer can establish a tradeoff between length of the amplitude intervals and duration of transients.

A. VALIDATION

As stated in the previous sections there is a series of hypotheses that must be verified in order that all points on the calculated bifurcation frontier be correct. Though the designer need to validate only the chosen control parameter combination, it would be interesting to know whether the entire frontier is correct. Since the analytic verification of the hypotheses demands a prohibitive effort, we opt to validate our analysis using numerical simulations. Among the cited hypotheses are: the unimodal limit cycle is a global behavior; the sufficiency of limit cycle stability condition; the absence of intermediary switches; the uniqueness of the stable limit cycle.

In order to check the validity of the limit cycle $\omega_0 < \omega_{\max}$ region we calculate via simulation the average time T

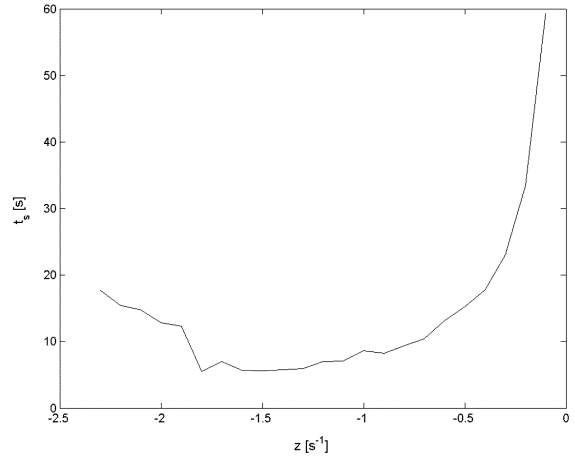

Fig. 13. Maximum roll angle settling time along the bifurcation frontier

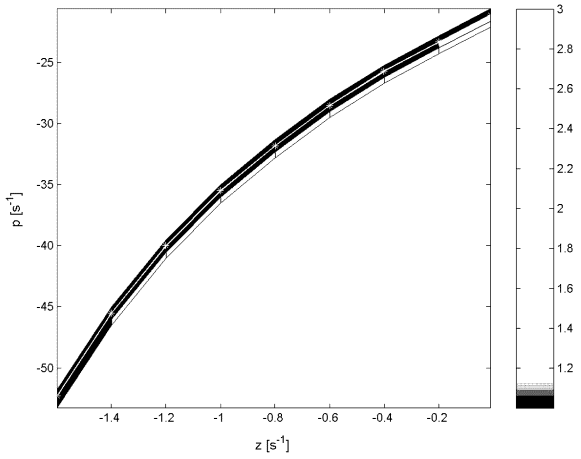

Fig. 14. Lyapunov dimension (grayscale) in the neighborhood of the bifurcation frontier (white line with stars)

between actuators positive switches. In the unimodal periodic case, this average corresponds to the period, that must satisfy $T \geq T_{\max}$. For complex periodic or non-periodic motions, we must have $T \leq T_{\max}$. The analysis of these conditions in the space $\alpha \times \tau$ has confirmed the validity of the region of robust limit cycle with $\omega_0 < \omega_{\max}$. Notice, however, that this analysis is well-suited to the open region but may not identify the bifurcation frontier precisely, since nothing can be said when $T = T_{\max}$. The variance of the times between positive switches would not suffice to identify the bifurcation frontier either, given that this variance may be very small for quasi-periodic-like motions in the neighbourhood of bifurcation.

Therefore, the strategy for validation of the frontier considers the Lyapunov dimension, given that Lyapunov exponents are important indicators of the occurrence of bifurcations [19]. Indeed, as they have unbounded variations in bifurcation points, these points can be accurately identified. For each point (z, p) in the bifurcation frontier neighborhood and for each point in a grid of α and τ, the validation procedure consists of the random choice of an initial condition and subsequent simulation of the system. Then, Lyapunov exponents are calculated using the method proposed by Müller [16], [20] to deal with discontinuous flow systems. Once dimensions greater than 1.05 are found, the search in the space $\alpha \times \tau$ may be interrupted and the motion is classified as non-periodic. The resulting dimensions are exhibited in Fig. 14 and confirm that the bifurcation frontier based on a parametric approach is very close to the actual frontier. This validation is carried just in a small neighborhood of the bifurcation frontier, for the calculation of the Lyapunov spectrum takes an excessively long time. Hence, both validations are complementary.

VII. Conclusion

In this paper we presented a study of the robust limit cycle control in an attitude control system with relay-type actuators subject to minimally spaced transition times. As the emergence of bifurcations in this system can seriously affect performance, we developed analysis/synthesis techniques for robust prevention of bifurcations and efficient employment of actuators. First-order linear controllers that robustly reduce both amplitude and fuel consumption can be obtained. However, the designer should establish a tradeoff between amplitude interval and transient duration. Tsypkin's method is used to investigate the robustness of the existence condition for time-constrained limit cycles. This allows the identification of a robustness frontier in the space of control parameters. Thus, reduced amplitude and fuel consumption can be obtained through the solution of a maximin problem for the oscillation frequency on this frontier. In addition, since most relay control systems are subject to similar time restrictions, the presented techniques may be useful to efficiently exploit actuators in other systems that alternate among unstable dynamics.

The proposed techniques introduce a robust limit cycle control that relies in exact limit cycle prediction. The discussed attitude control problem is an important instance for which an exact prediction would be noticeably advantageous in obtaining an improved performance. The main advantages in the use of exact methods are their accuracy and smaller conservativeness when compared to strategies that use the describing function and that take into account the contribution due to higher harmonics as an uncertainty. A disadvantage of exact methods in relation to the describing function methods is the low availability of control synthesis procedures. Other problems may arise in the case of systems of greater order, for a large number of stable limit cycles may occur. We believe that both of these deficiencies can be corrected through a joint analysis that uses describing function and exact methods. Moreover, we remark that similar techniques can also be applied in the design of frequency and amplitude bounded limit cycles.

An interesting improvement of the controller structure may be obtained by varying the minimum required rest between operations of different thrusters. This additional degree of

freedom can lead to a reduction in fuel consumption. We believe that a more elaborated version of the procedures in this paper would be able to address the problem.

REFERENCES

[1] J. Mendel, "On-off limit-cycle controllers for reaction-jet-controlled systems," *IEEE Transactions on Automatic Control*, vol. 15, no. 3, pp. 285–299, 1970.

[2] N. N. Antropov, G. A. Diakonov, M. N. Kazeev, V. P. Khodnenko, V. Kim, G. A. Popov, and A. I. Pokryshkin, "Pulsed plasma thrusters for spacecraft attitude and orbit control system," in *Proc. of the 26th International Propulsion Conference*, Japan, 1999, pp. 1129–1135.

[3] G. Avanzini and G. Matteis, "Bifurcation analysis of attitude dynamics in rigid spacecraft with switching control logics," *Journal of Guidance, Control, and Dynamics*, vol. 24, no. 5, pp. 953–959, 2001.

[4] N. M. Oliveira and K. H. Kienitz, "Attitude controller design for a system using actuators with switching-time restrictions and delays," in *AIAA Guidance, Navigation, and Control Conference*, Denver, 2000, pp. Paper AIAA–2000–3967.

[5] C. Won, "Comparative study of various control methods for attitude control of a leo satellite," *Aerospace Science and Technology*, vol. 3, no. 5, pp. 323–333, 1999.

[6] A. R. Mesquita and K. H. Kienitz, "Persistent motion and chaos in attitude control with switching actuators," in *16th IFAC World Congress*, Prague, 2005, pp. Paper Th–A03–TP/15.

[7] J. E. Tierno, "Describing function analysis in the presence of uncertainty," *Journal of Guidance, Control, and Dynamics*, vol. 20, no. 5, pp. 956–961, 1997.

[8] M. Fadali and N. Chachavalvoong, "Describing function analysis of uncertain nonlinear systems using the kharitonov approach," in *Proc. of the American Control Conference*, Seattle, pp. 2098–2912.

[9] Y. J. Huang, T. C. Kuo, and H. K. Lee, "Robust limit cycles suppression for control systems with parametric uncertainty and nonlinearity," *Nonlinear Dynamics*, vol. 35, no. 4, pp. 397–407, 2004.

[10] P. Nataraj and J. Barve, "Reliable and accurate algorithm to compute the limit cycle locus for uncertain nonlinear systems," *IEE Proceedings - Control Theory and Applications*, vol. 150, no. 5, pp. 457–466, 2003.

[11] ——, "New approach to assessing the effects of parametric variations in feedback loops," *IEE Proceedings - Control Theory and Applications*, vol. 150, no. 2, pp. 101–111, 2003.

[12] C. Fang and E. H. Abed, "Robust feedback stabilization of limit cycles in pwmdc-dc converters," *Nonlinear Dynamics*, vol. 27, no. 3, pp. 295–309, 2002.

[13] T. Leephakpreeda, "H-inf stability robustness of fuzzy control systems," *Automatica*, vol. 35, no. 8, pp. 1467–1470, 1999.

[14] M. Katebi and Y. Zhang, "H-inf control analysis and design for nonlinear systems," *International Journal of. Control*, vol. 61, no. 2, pp. 459–474, 1995.

[15] J. C. Gille, P. Decaulne, and M. Pélegrin, *Mthodes Dtude des Systmes Asservis Non Linaires*. Paris: Dunod, 1967.

[16] A. R. Mesquita, E. L. Rempel, and K. H. Kienitz, "Bifurcation analysis of attitude control systems with switching-constrained actuators," *Nonlinear Dynamics*, vol. 51, pp. 207–216, 2008.

[17] Y. Z. Tsypkin, *Relay Control Systems*. Cambridge, UK: Cambridge University Press, 1984.

[18] K. J. Astrom, *Adaptive Control, Filtering, and Signal Processing*, ser. The IMA Volumes in Mathematics and its Applications. New York: Springer-Verlag, 1995, vol. 74, ch. Oscillations in Systems with Relay Feedback.

[19] J. P. Eckmann and D. Ruelle, "Ergodic theory of chaos and strange attractors," *Reviews of Modern Physics*, vol. 57, no. 3, pp. 617–656, 1985.

[20] P. Muller, "Calculation of lyapunov exponents for dynamic systems with discontinuities," *Chaos, Solitons & Fractals*, vol. 5, no. 9, pp. 1671–1681, 1995.